Thermal annealing of GaN implanted with Be

M. A. Reshchikov,[a] O. Andrieiev,[a] M. Vorobiov,[a] D. Ye,[a] D. O. Demchenko,[a]
K. Sierakowski,[b] M. Bockowski,[b] B. McEwen,[c] V. Meyers,[c] and F. Shahedipour-Sandvik [c]

[a] *Department of Physics, Virginia Commonwealth University, Richmond, VA 23220, USA*

[b] *Institute of High Pressure Physics, Polish Academy of Sciences, Sokolowska 29/37, Warsaw 01-142, Poland*

[c] *College of Nanoscale Science and Engineering, SUNY Polytechnic Institute, Albany NY 12203, USA*

Abstract

GaN samples were implanted with Be and annealed in different conditions in order to activate the shallow Be_{Ga} acceptor. Low-temperature photoluminescence spectra were studied to find Be_{Ga}-related defects in the implanted samples. A yellow band with a maximum at about 2.2 eV (the YL_{Be} band) was observed in nearly all samples protected with an AlN cap during the annealing and in samples annealed under ultrahigh N_2 pressure. A green band with a maximum at 2.35 eV (the GL2 band), attributed to the nitrogen vacancy, was the dominant defect-related luminescence band in GaN samples annealed without a protective AlN layer. The ultraviolet luminescence (UVL_{Be}) band with a maximum at 3.38 eV attributed to the shallow Be_{Ga} acceptor with the ionization energy of 0.113 eV appeared in implanted samples only after annealing at high temperatures and ultrahigh N_2 pressure. This is the first observation of the UVL_{Be} band in Be-implanted GaN, indicating successful activation of the Be_{Ga} acceptor.

INTRODUCTION

The production of high-quality *p*-type GaN by ion implantation remains a challenge. Currently, the only *p*-type dopant in GaN is Mg. However, relatively high ionization energy (0.22 eV) of the Mg_{Ga} acceptor requires high doping concentrations to achieve *p*-type conductivity suitable for practical applications. It is expected that doping of wide-bandgap nitrides such as GaN,[1,2,3,4,5] AlN,[6,7] BN,[8] and their alloys with Be may produce high-conductivity *p*-type materials and cause a breakthrough in the development of bright UV emitters. First-principles calculations predict that Be_{Ga} in GaN is a deep acceptor with the ionization energy $E_A \approx$ 450-550 meV.[9,10] However, photoluminescence (PL) studies provide strong evidence for the Be-related acceptor level at ~0.1 eV above the valence band in Be-doped GaN.[1,11,12,13,14,15,16]

Recently, we showed that Be in GaN exhibits a shallow acceptor state at 113±5 meV above the valence band, which is responsible for a PL band (labeled UVL_{Be}) with a sharp peak at 3.38 eV, followed by a series of LO phonon replicas.[1] The UVL_{Be} band is often observed in Be-doped GaN layers grown by molecular beam epitaxy (MBE).[1,11,12,14,15,16] However, we are not aware of any work in which the UVL_{Be} band was observed in GaN after implantation with Be. The reason may include the low mobility of Be in GaN and the low fraction of Be substituting for Ga atoms.[17,18]

Post-implantation annealing is necessary to remove crystal defects such as vacancies and vacancy complexes. For GaN, to recover from the ion implantation damage, the annealing temperature, T_{ann}, should be well above 1000 °C.[19,20] However, decomposition of GaN begins at $T_{ann} \approx$ 900 °C in N_2, Ar, or He ambient under atmospheric pressure.[21,22] In H_2 ambient, the decomposition starts already at 800 °C.[22] Higher annealing temperatures can be achieved by

employing an AlN cap layer, yet the GaN decomposition is still observed at 1200 °C.[23] To resolve the problem, ultra-high-pressure-annealing (UHPA) of GaN has been recently proposed.[24] Sakurai *et al*.[25] demonstrated that cap-free annealing of Mg-implanted GaN under a nitrogen pressure of 1 GPa at T_{ann} = 1200 − 1480 °C removes implantation-induced crystal damage and activates Mg acceptors without thermal decomposition of GaN. At such high temperatures, the diffusion of implanted species and other impurities may also be significant.[25]

There is limited research on the Be diffusion in GaN. Early studies demonstrated no significant diffusion of Be during rapid thermal annealing (RTA) at temperatures up to 1200 °C.[26,27] Koskelo *et al*.[28] investigated the Be diffusion at 850 and 950 °C by annealing for six days and 2.5 hours, respectively, under Ar-gas atmosphere after ion implantation of ^{7}Be and ^{7}Li ions. Jakiela *et al*.[17] studied the Be diffusion at temperatures between 1200 and 1400 °C under UHPA in nitrogen ambient during 15-30 min after ^{9}Be implantation to GaN with very low density of dislocations. They concluded that the Be diffusion occurs by two mechanisms: rapid interstitial and slow interstitial-substitutional diffusion. By combining the experimental data from these two works, we conclude that the diffusion coefficient D for Be in GaN varies with temperature as [17,28]

$$D = D_0 \exp\left(\frac{-E_A}{kT}\right). \quad (1)$$

with pre-exponential factor $D_0 \approx 0.01$ and the activation energy $E_A \approx 2.8$ eV.

In this work, we demonstrate that activation of the Be_{Ga} acceptors in Be-implanted GaN can be successfully achieved by post-implantation annealing at high temperatures and ultra-high nitrogen pressure.

I. EXPERIMENTAL DETAILS

Nominally undoped GaN layers were grown on sapphire and ammonothermal GaN (Am-GaN) substrates by halide vapor phase epitaxy (HVPE) (Table I). The samples were implanted at room temperature with different doses and energies of $^{9}Be^{+}$ ions at a 7° tilt angle. Samples of series E were additionally implanted with ^{14}N. After the implantation, the samples were annealed in different conditions. Samples of series A-D were cut into 5×5 mm squares and annealed in N_2 ambient at temperatures from 950 to 1100 °C for 1-4 h, by RTA at 900-1225 °C for 1.5-2 min, or under ultrahigh N_2 pressure (1 GPa) at temperatures from 1250 to 1400 °C. In some cases, a protective ~80 nm-thick AlN cap layer was deposited onto the sample surface before the annealing. Samples of series E were annealed by the UHPA method at T_{ann} = 1250 – 1400 °C without any protective layer.

TABLE I. Implantation parameters

Sample series	HVPE GaN thickness (μm)	Substrate	^{9}Be energy (keV)	^{9}Be dose (cm^{-2})	^{14}N energy (keV)	^{14}N dose (cm^{-2})	[Be] [a)] (cm^{-3})
A	5	Sapphire	40	10^{12}	-	-	~10^{16}
B	5	Sapphire	40	10^{13}	-	-	~10^{17}
C	5	Sapphire	180	10^{13}	-	-	~10^{16}
D	5	Sapphire	40	10^{14}	-	-	~10^{18}
E	50	Am-GaN	500	2×10^{15}	500	2×10^{15}	~10^{18}

[a)] The concentration of Be in the near-surface 200 nm-thick layer estimated from SRIM simulations and SIMS measurements on selected samples

Steady-state PL was excited with a HeCd laser. Other details of PL experiments can be found elsewhere.[29,30] The as-measured PL spectra were corrected for the measurement system's spectral response, and PL intensity was additionally multiplied by λ^3, where λ is the light

wavelength, to present the PL spectra in units proportional to the number of emitted photons as a function of photon energy.[29] For selected samples, PL spectra were also measured before and after implantation (before any annealing experiments). The original HVPE GaN samples from Kyma showed typical for such material PL spectra with weak RL1, YL1, GL1, and UVL bands.[30] After ion implantation, the PL signal from samples of series B, C, and D dropped by at least three orders of magnitude, and no PL bands could be recognized. In samples implanted with the lowest Be dose (series A), the RL1, YL1, and UVL bands could be resolved with intensities by order of magnitude lower than in as-grown samples.

We assume that PL signal is collected from the depth of up to ~200 nm, which is limited by significant light absorption at 325 nm and small charge carrier diffusion length in Be-implanted GaN samples. From the SRIM Monte Carlo simulations, the depth profile of Be is expected to have a maximum at 125, 500, and 1100 nm for Be ion energies of 40, 180, and 500 keV, respectively. The concentration of Be in the maximum is expected to be 7×10^{16}, 7×10^{17}, 3.5×10^{17}, 7×10^{18}, and 5×10^{19} cm^{-3} for samples from series A, B, C, D, E, respectively. For samples of Series E, the implantation profiles after annealing are expected to be similar to those in samples implanted with Be and annealed in similar conditions.[17] The depth profiles were also measured for selected samples using secondary ion mass spectrometry (SIMS). Only for samples of series D (with the implantation dose of 10^{14} cm^{-2}) the presence of Be with the concentration of $1\text{-}5\times10^{18}$ cm^{-3} in the near-surface region up to ~200 nm could be reliably found. For other samples (series A-C), the concentration of Be was close to or below the detection limit (10^{16} -10^{17} cm^{-3}). In the last column of Table I, a rough estimate (order of magnitude) for the concentration of Be in the near-surface 200 nm-thick layer is presented based on combined information from the SRIM simulations and SIMS measurements.

II. RESULTS AND DISCUSSION

A. Be-related PL bands in GaN:Be

PL bands from defects in GaN have reproducible features such as PL band shape, the temperature dependence of PL intensity, PL lifetime, electron- and hole-capture coefficients.[30] These features serve as fingerprints to identify defects or recognize the PL bands caused by unknown defects. In this section, we will briefly review the main features of defects observed in Be-doped GaN grown by MBE.[1,31]

Figure 1 shows the main defect-related PL bands in MBE GaN:Be samples.[31] At low temperature (18 K), three Be-related PL bands are observed: the UVL_{Be} band with the main peak at 3.38 eV followed by several LO phonon replicas, the broad YL_{Be} band with a maximum at 2.15 eV, and the RL_{Be} band with a maximum at 1.8 eV (Fig. 1). In samples with the strong RL_{Be} band, we also observed the GL2 band with a maximum at 2.33 eV. The shapes of the broad PL bands can be fitted with the following expression obtained in a one-dimensional configuration coordinate model.[32]

$$I^{PL}(\hbar \qquad \hbar \qquad \left[-2S_e \left(\sqrt{\frac{E_0^* - \hbar}{d_{FC}^g}} \qquad 1 \right)^2 \right]. \qquad (2)$$

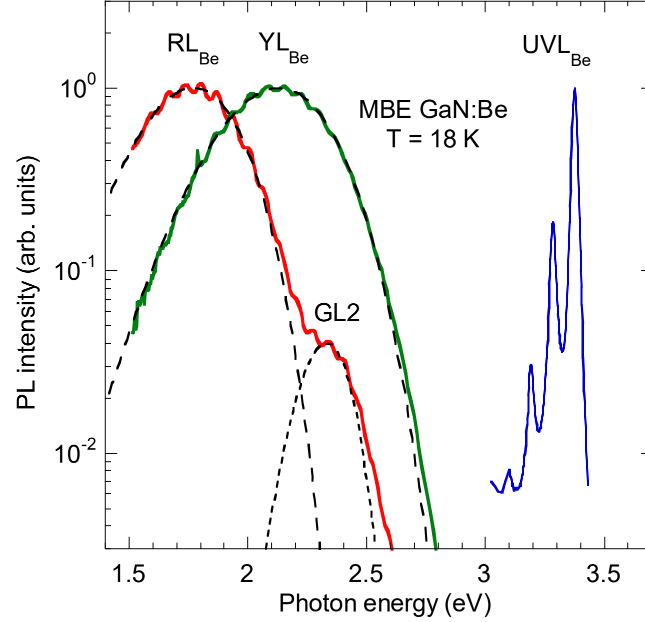

Fig. 1. Defect-related PL bands (normalized intensity) observed in Be-doped GaN. The PL spectra are from three GaN:Be samples grown by MBE. The dashed lines show the shapes of the RL_{Be}, YL_{Be}, and GL2 bands calculated by using Eq. (2) with parameters in Table II.

Here, S_e is the Huang-Rhys factor in the excited state of the defect, $d_{FC}^{g} = E_0^{*} - \hbar$ is the Frank-Condon shift in the ground state, $E_0^{*} = E_0 + 0.5\hbar$, E_0 is the zero-phonon line (ZPL) energy, $\hbar$ is the energy of the effective phonon mode in the excited state, $\hbar$ and $\hbar$ are the photon energy and position of the PL band maximum, respectively. The Δ is a small shift of the PL band maximum due to sample-dependent reasons such as in-plane biaxial strain in thin GaN layers grown on sapphire substrates. According to Eq. (2), the shape of a PL band with a maximum at $\hbar$ depends only on parameters S_e and d_{FC}^{g}. Table II presents these parameters for the broad PL bands in Be-doped GaN and updated parameters for other PL bands commonly observed in undoped GaN.

TABLE II. Main PL bands in Be-doped GaN (first two rows) and in undoped GaN, parameters defining the bands' positions and shapes, ZPL (when observed), and the charge transition level above the top of the valence band (E_A).

PL band	Preliminary attribution	$\hbar$ (eV)	S_e	E_0^* (eV)	ZPL (eV)	E_A (eV)
RL_{Be}	$Be_{Ga}V_N$	1.77	~20	~2.6	-	~0.9
YL_{Be}	Be_{Ga} complex	2.15	24	3.2	-	0.3
RL1	Cl-related?	1.73	9.5	2.3	-	~1.2
RL2	V_N complex	1.72	~23	~2.5	-	~0.9
YL1	C_N	2.17	7.8	2.67	2.59	0.916
YL3	Fe-related	2.07	6.2	2.41	2.38	1.130
GL1	Unknown	2.35	10.3	2.97	-	~0.5
GL2	V_N	2.33	26.5	2.85	-	~0.45
BL1	Zn_{Ga}	2.86	3.2	3.14	3.10	0.400
BL2	C_NH_i	3.0	4.6	3.38	3.33	0.150

The parameters of the YL_{Be} band and the C_N-related yellow band (labeled YL1) differ, although positions of their maxima coincide. The PL bands are also different in terms of other properties. The YL1 band in *n*-type GaN quenches at temperatures above 500 K due to thermal emission of holes from the –/0 level of the C_N acceptor at 0.9 eV above the valence band.[33] The quenching of the YL_{Be} band in *n*-type GaN:Be begins at 200 K, and the activation energy of this quenching is 0.3 eV.[31] We preliminarily proposed that the $Be_{Ga}V_NBe_{Ga}$ complex with a ground state at ~1.5 eV and an excited state at 0.3 eV above the valence band is responsible for the YL_{Be} band in MBE-grown GaN:Be.[31] Teisseyre *et al*. attributed the yellow band in bulk Be-doped GaN grown by the high-nitrogen-pressure-solution method to the $Be_{Ga}O_N$ complex.[34] Note that the YL_{Be}

band in the MBE GaN and yellow band in bulk GaN:Be are apparently caused by different defects.[31] In particular, the quenching of the yellow band in bulk GaN:Be begins only at T >500 K.[35]

The shape of the UVL_{Be} band in GaN is unique. This defect has the smallest Huang-Rhys factor (the ratio of the first phonon replica intensity to the ZPL intensity) and the shallowest energy level (E_A = 113±5 meV) among defects in GaN. We attribute this band to the shallow state of the Be_{Ga} acceptor, while the deep state is not observed in PL experiments, possibly due to the low hole-capture cross-section.[1]

In MBE-grown GaN:Be samples studied in Refs. 1 and 31, the UVL_{Be} and YL_{Be} bands were the main defect-related bands, whereas the RL_{Be} band was strong only in samples also containing the GL2 band (Fig. 1). The GL2 band can be easily recognized by a relatively narrow width, Gaussian shape, and exponential decay of PL after a laser pulse, with a characteristic lifetime of 250 μs.[32] The GL2 and RL_{Be} bands are attributed to the isolated nitrogen vacancy (V_N) and its complex with Be_{Ga}, respectively.[31,32] The $Be_{Ga}V_N$ complex is a deep donor with the ground 0/+ level at about 2.5 eV below the conduction band and an excited state close to the conduction band. In time-resolved PL experiments, this band can be recognized by an exponential decay with the characteristic time of 2 μs at T = 18 K.[31] It may be difficult to distinguish the RL_{Be} band in Be-doped GaN and the RL2 band in semi-insulating undoped GaN samples.[36] A detailed study of the V_N-related red PL bands in GaN will be presented elsewhere.[37] In contrast, the YL_{Be} and UVL_{Be} bands have specific properties that allow us to recognize them confidently.

As a result of ion implantation and post-implantation thermal annealing, various defects are created. The Be atoms may substitute for Ga, N, occupy interstitial positions, or form

complexes. We searched for the UVL_{Be} and YL_{Be} bands in PL spectra as signatures of the Be_{Ga} defects. In particular, the Be_{Ga}-related UVL_{Be} band has never been observed in GaN implanted with Be before, while this shallow acceptor state is often observed in Be-doped GaN grown by MBE.

B. Annealing in nitrogen under atmospheric pressure

Low-temperature PL spectra from as-grown HVPE GaN layers on sapphire substrates contained intense excitonic lines and defect-related PL bands typical for this material: the RL1, YL1, BL1, and UVL bands (Table I). By using the approach described in Refs. 38 and 39, we estimated the concentrations of related defects as 6×10^{15}, 1.5×10^{15}, 1.5×10^{13}, and 7×10^{12} cm^{-3}, respectively. A weak GL1 band can also be resolved in these PL spectra at high excitation intensities. After Be implantation, the PL from GaN samples became very weak, with total radiative efficiency lower than 10^{-4}. The exciton emission was 10^4 times weaker than in material before implantation, and no familiar defect-related PL bands could be found.

Samples of series A-D, after Be implantation, were annealed under atmospheric pressure in N_2 ambient at temperatures between 950 and 1100 °C in different conditions, including RTA and long annealing, with and without an 80-nm-thick AlN cap. The PL spectra were studied in detail for all these samples, and the main results are presented below.

1. Annealing of GaN with a bare surface

In the first annealing experiments, samples from series A-D were annealed after Be ion implantation without AlN cap for two hours in N_2 ambient at temperatures from 950 to 1100 °C with a step of 50 °C. We could not find the YL_{Be} and UVL_{Be} bands in these samples. Representative

PL spectra for T_{ann} = 1000 °C are shown in Fig. 2a. In this and the following figures, PL intensities are presented in the same relative units.

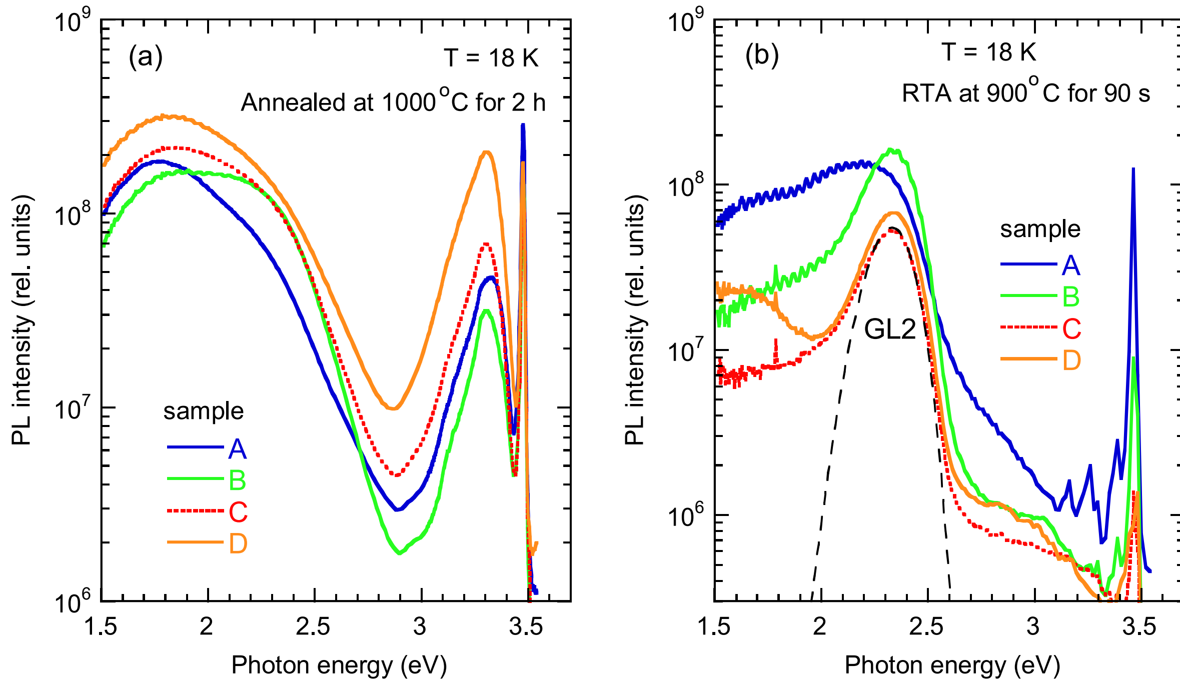

Fig. 2. PL spectra from GaN samples implanted with Be and annealed without AlN cap. (a) Annealing in atmospheric-pressure N_2 at 1000 °C for 2 hours. (b) RTA at 900 °C for 90 s. The GL2 band is caused by the isolated V_N. All the measurements were done in identical conditions.

In addition to excitonic emission with a maximum at 3.47 eV (by a factor of 100 weaker than in the samples before the irradiation), a structureless band was observed in the UV region. This band markedly shifts with excitation intensity (from ~3.2 to 3.4 eV with increasing excitation intensity, P_{exc}, from 10^{-4} to 100 W/cm^2). Although this band's position roughly matches the UVL_{Be} band's position, no characteristic fine structure could be revealed. We attribute this band to diagonal transitions from the conduction band to the valence band in regions with large potential

fluctuations in semi-insulating material.[30] Another broad PL band at lower photon energies consists of at least two bands. The origin of the red band at ~1.8 eV could not be established, whereas the band at ~2.35 eV was identified as the GL2 band caused by the V_N defect.

Samples from series A-D without AlN cap were also annealed by RTA for 90 s in N_2 at T_{ann} = 900 °C. The GL2 band was the dominant defect-related PL band in these samples (Fig. 2b). We conclude that the V_N defects are formed abundantly at these temperatures when GaN is annealed without a protective cap layer. Note that the GL2 band is not observed in conductive *n*-type GaN. This is because the Fermi level in such samples is located above the 0/+ level of the V_N, and the capture of photogenerated holes by the neutral V_N is very inefficient.

2. Annealing of GaN with AlN cap

In the following experiments, 80-nm-thick AlN films were deposited on the samples from series A-D to prevent GaN decomposition. These samples were annealed at 1100 °C for 1 and 4 hours and alternatively at 1225 °C by RTA. Typical PL spectra from these samples are shown in Fig. 3. The YL_{Be} band was the dominant defect-related band in the samples annealed at relatively high temperatures with an AlN cap. The V_N-related GL2 band was observed in some samples. It could be better resolved at low excitation intensities and at temperatures close to 200 K when the YL_{Be} band is quenched. No UVL_{Be} band could be found in these samples. Rarely, a weak Mg-related UVL band (UVL_{Mg}) with a maximum at ~3.27 eV was observed in this spectral region (Fig. 3a).

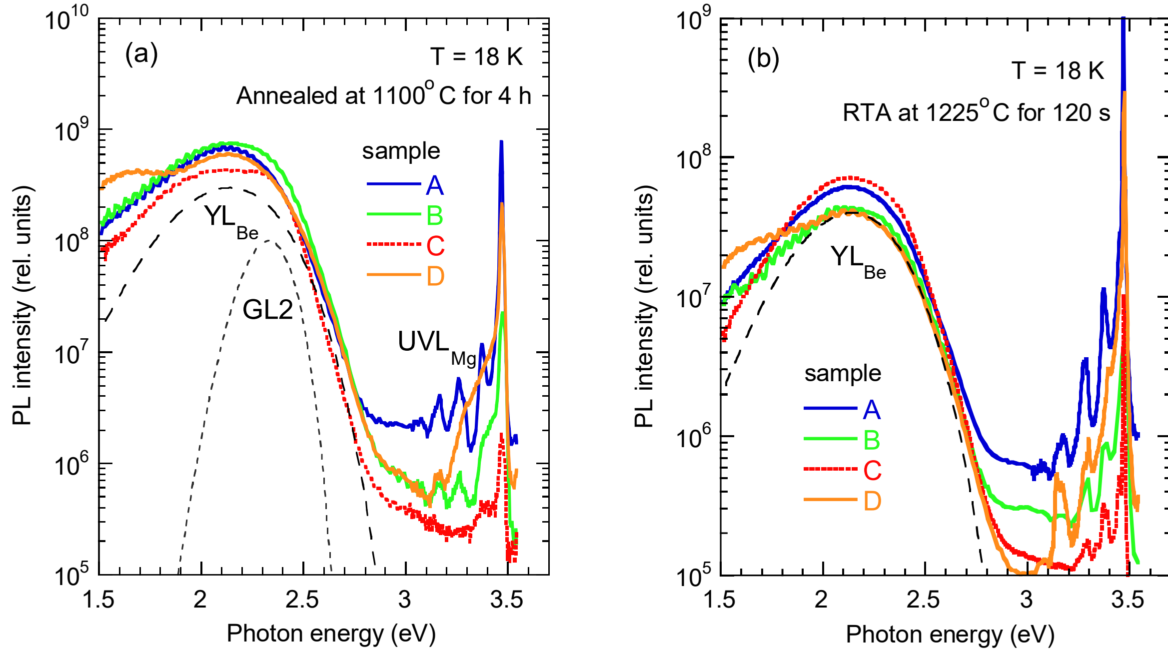

Fig. 3. PL spectra from GaN implanted with Be, covered with protective AlN cap, and annealed in N_2 at atmospheric pressure. (a) Samples annealed at 1100 °C for 4 hours. (b) Samples annealed by RTA at 1225 °C for 120 s. The dashed lines show the shapes of the YL_{Be} and GL2 bands calculated using Eq. (2) with parameters given in Table II.

C. Annealing under ultrahigh N_2 pressure

1. Samples of series A-D treated by UHPA

The Be-implanted GaN samples of series A-D were also annealed at high temperatures (1250-1400 °C) under ultrahigh N_2 pressure to avoid the decomposition of GaN. Representative PL spectra for the highest annealing temperature are shown in Fig. 4. Similar trends were observed for all other T_{ann}.

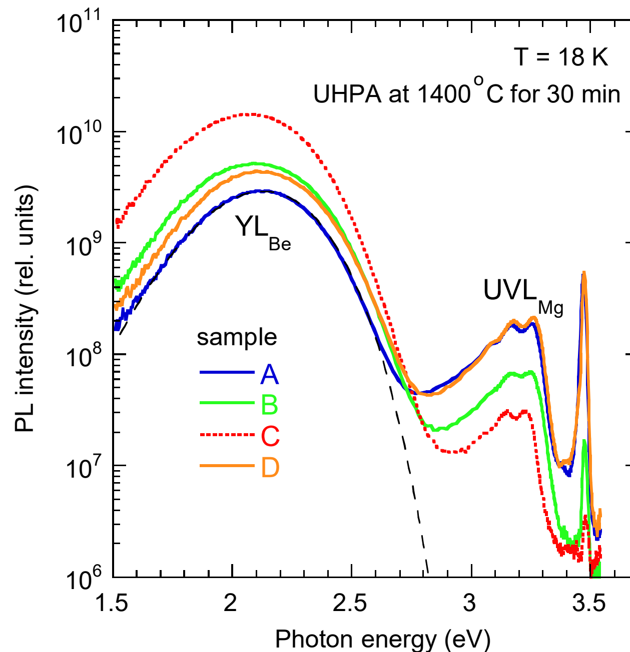

Fig. 4. PL spectra from GaN samples implanted with Be and annealed under ultrahigh N_2 pressure (1 GPa) at 1400 °C for 30 min.

The YL_{Be} intensity significantly increased compared to the samples annealed at lower temperatures and atmospheric pressure (Fig. 3). The YL_{Be} band peak intensity of $\sim 10^{10}$ in this and other figures roughly corresponds to the quantum efficiency close to unity according to our calibrations.[30] For samples implanted with the same Be^+ ion energy (40 keV), we consistently observed a proportional decrease of the exciton emission intensity with the implantation dose increase and a monotonous increase of the YL_{Be} intensity (the increase could not be linearly proportional because its quantum efficiency approached unity). With increasing T_{ann} from 1250 to 1400 °C, for each series of samples in the group A-D, the YL_{Be} intensity monotonously increased (totally by a factor of 1.5-3). Since the YL_{Be} band is caused by Be_{Ga}-related defects,[31,34] the significant increase of its intensity indicates activation of the Be_{Ga} after UHPA.

Interestingly, the Mg-related UVL_{Mg} band appeared in the PL spectra of samples annealed using the UHPA method. We observed a relatively intense UVL_{Mg} band in all samples annealed by this method. The UVL_{Mg} band intensity monotonously increased with increasing T_{ann} for each implantation set (totally by about an order of magnitude for T_{ann} varied from 1250 to 1400 °C). The Mg likely originates from GaN powder covering the samples during UHPA. With increasing T_{ann}, diffusion of Mg to the Be-implanted samples increases. While the quantum efficiency of the YL_{Be} band approaches unity in some UHPA-treated samples, that of the UVL_{Mg} band remains below ~0.02, which corresponds to the concentrations of Mg lower than 10^{15} cm^{-3} (Ref. 39).

2. Samples of series E treated by UHPA

Samples of series E were co-implanted with Be and N. The purpose of the implantation with nitrogen ions was to reduce the formation of the V_N. It is known that sequential implantation of Mg and N ions into GaN improves the Mg_{Ga} acceptor activation and significantly decreases the contribution of the V_N-related GL2 band in the PL spectrum.[40,41,42] Note that similar effects have been observed for GaN implanted at high temperature with Mg and F.[43]

Representative PL spectra are shown in Fig. 5. In this sample set, the YL_{Be} band overlaps with a red PL band of unknown origin. The measurements of PL spectra in a wide range of temperatures revealed the V_N-related GL2 band only in samples annealed at 1250 and 1300 °C (in Fig. 5, the GL2 band contribution in the spectrum from the sample annealed at 1250 °C is shown with a dashed curve). Remarkably, the UVL_{Be} band was observed in all GaN samples co-implanted with Be and N. The highest intensity of this band was achieved in the sample annealed at 1300 °C (Fig. 5). One of the samples was implanted with only Be under the same conditions as other samples of series E and annealed by UHPA at 1400 °C. There was no significant difference in PL spectra between this sample and the sample co-implanted with Be and N and annealed at 1400 °C.

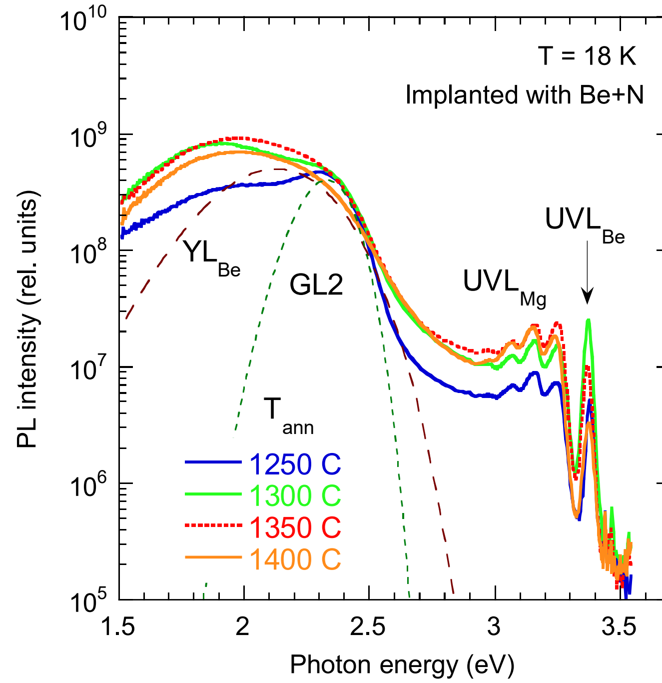

Fig. 5. PL spectra from GaN samples of series E co-implanted with Be and N and annealed under ultrahigh N_2 pressure (1 GPa) for 30 min. $P_{exc} = 0.005$ W/cm^2.

The relative contribution of the UVL_{Be} band to PL spectra increased with increasing excitation intensity because the broad bands at photon energies below 3 eV could be easily saturated, whereas the UVL_{Be} band intensity increases superlinearly with P_{exc}.[31] PL spectra in the UV region obtained with a focused HeCd laser beam ($P_{exc} \approx 100$ W/cm^2) are shown in Fig. 6. The main peak of the UVL_{Be} band at 3.38 eV is followed by LO phonon replicas at distances multiple of 92 meV. These replicas overlap with the main peak of the UVL_{Mg} band at 3.27 eV, also followed by LO phonon replicas. As can be seen from this figure, the relative intensity of the UVL_{Be} band decreases significantly in samples annealed at $T_{ann} > 1300$ °C. Interestingly, the intensity of this band in the sample implanted with only Be remains high for $T_{ann} = 1400$ °C.

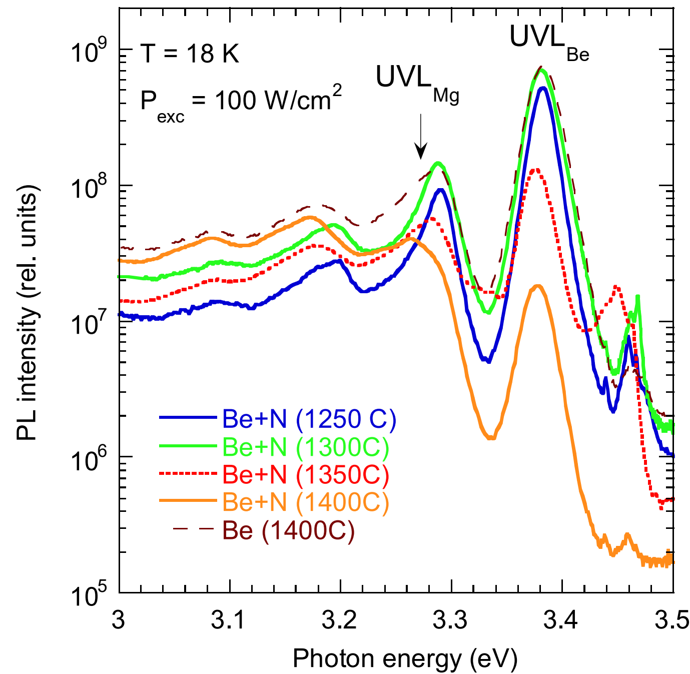

Fig. 6. PL spectra from GaN samples of series E co-implanted with Be and N (one sample is implanted with Be only) and annealed under ultrahigh N_2 pressure (1 GPa) for 30 min. $P_{exc} \approx$ 100 W/cm^2. The relative units in this figure cannot be compared to the relative units in Figs. 2-5 because conditions for collection PL were not the same for unfocused and focused laser beams.

This is the first observation of the Be_{Ga}-related UVL_{Be} band in GaN implanted with Be to the best of our knowledge. Previously, this band was observed only in Be-doped GaN. It is not clear why the UVL_{Be} band appeared in samples of series E but was not observed in samples of series A-D annealed in the same conditions by UHPA. The samples of series E were implanted with a higher dose and energy of Be ions (Table I). They are also expected to have much lower dislocation density because the HVPE layers were grown on bulk ammonothermal GaN templates as opposed to sapphire substrates for the series A-D. No electrical measurements have been conducted so far on the studied samples. However, the observation of the GL2 band indicates that the samples are

semi-insulating. Further studies will explore optimal implantation and annealing conditions to find a route for efficient *p*-type GaN.

III. CONCLUSION

In MBE-grown GaN samples doped with Be, the PL spectrum contains the UVL_{Be} band caused by the shallow Be_{Ga} acceptor and the YL_{Be} band caused by a Be-containing complex. We implanted Be into HVPE-grown GaN and annealed the implanted samples in different conditions. The YL_{Be} band was observed in nearly all samples protected with an AlN cap during the annealing and in samples annealed under ultrahigh N_2 pressure. The UVL_{Be} band was observed only after annealing at high temperatures and ultrahigh N_2 pressure. The ultra-high pressure annealing favors the formation of the Be_{Ga} acceptors, and thus it is a promising route for activating beryllium implanted in GaN.

ACKNOWLEDGEMENTS

The work at VCU and SUNY was supported by the National Science Foundation under grants DMR-1904861 and DMR-1905186, respectively. This research was also supported by the Polish National Science Center through project 2018/29/B/ST5/00338, as well as by the TEAM TECH program of the Foundation for Polish Science co-financed by the European Union under the European Regional Development Fund (POIR.04.04.00-00-5CEB/17-00). We would also like to thank Dr. K. Mizohata from the University of Helsinki and Dr. R. Jakiela from the Institute of Physics PAS for nitrogen and beryllium implantation to GaN samples (series E).

AUTHOR DECLARATIONS

Conflict of Interest

The authors have no conflicts to disclose.

DATA AVAILABILITY

The data supporting this study's findings are available from the corresponding author upon reasonable request.

References

[1] D. O. Demchenko, M. Vorobiov, O. Andrieiev, T. H. Myers, and M. A. Reshchikov, “Shallow and deep states of beryllium acceptor in GaN: Why photoluminescence experiments do not reveal small polarons for defects in semiconductors”, Phys. Rev. Lett. **126**, 027401 (2021).

[2] O. Brandt, H. Yang, H. Kostial, and K. H. Ploog, “High p-type conductivity in cubic GaN/GaAs(133)A by using Be as the acceptor and O as a codopant”, Appl. Phys. Lett. **69**, 2707-2709 (1996).

[3] S. Sugita, Y. Watari, G. Yoshizawa, J. Sodesawa, H. Yamamizu, K.-T. Liu, Y.-K. Su, and Y. Horikoshi, “Growth of Be-doped *p*-type GaN under invariant polarity conditions”, Jpn. J. Appl. Phys. **42**, 7194-7197 (2003).

[4] Y. Nakano, T. Kachi, and T. Jimbo, “Effect of Be^+ + O^+ co-implantation on Be acceptors in GaN”, Appl. Phys. Lett. **82**, 2082-2084 (2003).

[5] T. M. Al Tahtamouni, A. Sedhain, J. Y. Lin and H. X. Jiang, “Beryllium Doped *p*-type GaN Grown by Metal-Organic Chemical Vapor Deposition”, Jordan J. Physics **3**, 77-81 (2010).

[6] H. Ahmad, J. Lindemuth, Z. Engel, C. M. Matthews, T. M. McCrone, and W. A. Doolittle, “Substantial P-Type Conductivity of AlN Achieved via Beryllium Doping”, Adv. Mater. 2104497 (2021).

[7] R. Q. Wu, L. Shen, M. Yang, Z. D. Sha, Y. Q. Cai, Y. P. Feng, Z. G. Huang, and Q. Y. Wu, “Possible efficient *p*-type doping of AlN using Be: An *ab initio* study”, Appl. Phys. Lett. **91**, 152110 (2007).

[8] B. He, W. J. Zhang, Z. Q. Yao, Y. M. Chong, Y. Yang, Q. Ye, X. J. Pan, J. A. Zapien, I. Bello, S. T. Lee, I. Gerhards, H. Zutz, and H. Hofsäss, “*p*-type conduction in beryllium-implanted hexagonal boron nitride films”, Appl. Phys. Lett. **95**, 252106 (2009).

[9] S. Lany and A. Zunger, "Dual nature of acceptors in GaN and ZnO: The curious case of the shallow Mg_{Ga} deep state", Appl. Phys. Lett. **96**, 142114 (2010).

[10] J. L. Lyons, A. Janotti, and C. G. Van de Walle, "Impact of group-II acceptors on the electrical and optical properties of GaN", Jap. J. Appl. Phys. **52**, 08JJ04 (2013).

[11] F. J. Sánchez, F. Calle, M. A. Sánchez-Garcia, E. Calleja, E. Munoz, C. H. Molloy, D. J. Somerford, J. J. Serrano, and J. M. Blanco, "Experimental evidence for a Be shallow acceptor in GaN grown on Si(111) by molecular beam epitaxy", Semicond. Sci. Technol. **13**, 1130-1133 (1998).

[12] D. J. Dewsnip, A. V. Andrianov, I. Harrison, J. W. Orton, D. E. Lacklison, G. B. Ren, S. E. Hooper, T. S. Cheng and C. T. Foxon, "Photoluminescence of MBE grown wurtzite Be-doped GaN", Semicond. Sci. Technol. **13**, 500-504 (1998).

[13] M. Jaworek, A. Wysmolek, M. Kaminska, A. Twardowski, M. Bockowski, and I. Grzegory, "Photoluminescence study of bulk GaN doped with beryllium", Acta Phys. Pol. **108**, 705-710 (2005).

[14] A. Kawaharazuka, T. Tanimoto, K. Nagai, Y. Tanaka, and Y. Horikoshi, "Be and Mg co-doping in GaN", J. Cryst. Growth **301-302**, 414 (2007).

[15] H. Teisseyre, I. Gorczyca, N. E. Christensen, A. Svane, F. B. Naranjo, and E. Calleja, "Pressure behavior of beryllium-acceptor level in gallium nitride", J. Appl. Phys. **97**, 043704 (2005).

[16] K. Lee, B. L. VanMil, M. Luo, L. Wang, N.C. Giles, and T.H. Myers, "Thermal activation of beryllium-related photoluminescence by annealing of GaN grown by molecular beam epitaxy", Phys. Stat. Sol. C **2**, 2204–2207 (2005).

[17] R. Jakiela, K. Sierakowski, T. Sochacki, M. Iwinska, M. Fijalkowski, A. Barcz, and M. Bockowski, "Investigation of diffusion mechanism of beryllium in GaN", Physica B **594**, 412316 (2020).

[18] F. Tuomisto, V. Prozheeva, I. Makkonen, T. H. Myers, M. Bockowski, and H. Teisseyre, Phys. Rev. Lett. **119**, 196404 (2017).

[19] J. C. Zolper, "Ion implantation in group III-nitride semiconductors: a tool for doping and defect studies", J. Crys. Growth **178**, 157-167 (1997).

[20] A. Uedono, S. Takashima, M. Edo, K. Ueno, H. Matsuyama, H. Kudo, H. Naramoto, and S. Ishibashi, "Vacancy-type defects and their annealing behaviors in Mg-implanted GaN studied by a monoenergetic positron beam", Phys. Status Solidi B **252**, 2794–2801 (2015).

[21] H. W. Choi, M. G. Cheong, M. A. Rana, S. J. Chua, T. Osipowitz, and J. S. Pan, "Rutherford backscattering analysis of GaN decomposition", J. Vac. Sci. Technol. B **21**, 1080-1083 (2003).

[22] M. Mayumi, F. Satoh, Y. Kumagai, and A. Koukitu, "*In situ* gravimetric monitoring of decomposition rate from GaN (0001) and (000-1) surfaces using freestanding GaN", Jpn. J. Appl. Phys. **40**, L654-L656 (2001).

[23] J. D. Greenlee, B. N. Feigelson, T. J. Anderson, M. J. Tadjer, J. K. Hite, M. A. Mastro, C. R. Eddy Jr., K. D. Hobart, and F. J. Kub, "Multicycle rapid thermal annealing optimization of Mg-implanted GaN: Evolution of surface, optical, and structural properties", J. Appl. Phys. **116**, 063502 (2014).

[24] K. Sierakowski, R. Jakiela, B. Lucznik, P. Kwiatkowski, M. Iwinska, M. Turek, H. Sakurai, T. Kachi, and M. Bockowski, "High Pressure Processing of Ion Implanted GaN - MDPI", Electronics **9**, 1380 (2020)

[25] H. Sakurai, M. Omori, S. Yamada, Y. Furukawa, H. Suzuki, T. Narita, K. Kataoka, M. Horita, M. Bockowski, J. Suda, *and* T. Kachi, "Highly effective activation of Mg-implanted p-type GaN by ultra-high-pressure annealing", Appl. Phys. Lett. **115**, 142104 (2019).

[26] R. G. Wilson, J. M. Zavada, X. A. Cao, R. K. Singh, S. J. Pearton, H. J. Guo, S. J. Pennycook, M. Fu, J. A. Sekhar, V. Scarvepalli, R. J. Shu, J. Han, D. J. Rieger, J. C. Zolper, and C. R. Abernathy, "Redistribution and activation of implanted S, Se, Te, Be, Mg, and C in GaN", J. Vac. Sci. Technol. A **17**, 1226-1229 (1999).

[27] D. F. Storm, D. S. Katzer, S. C. Binari, E. R. Glaser, B. V. Shanabrook, and J. A. Roussos, "Reduction of buffer layer conduction near plasma-assisted molecular-beam epitaxy grown GaN/AlN interfaces by beryllium doping", Appl. Phys. Lett. **81**, 3819-3820 (2002).

[28] O. Koskelo, U. Köster, F. Tuomisto, K. Helariutta, M. Sopanen, S. Suihkonen, O. Svensk, and J. Räisänen, "Migration kinetics of ion-implanted beryllium in ZnO and GaN", Phys. Scr. **88**, 035603 (2013).

[29] M. A. Reshchikov, M. Vorobiov, D. O. Demchenko, Ü. Özgür, H. Morkoç, A. Lesnik, M. P. Hoffmann, F. Hörich, A. Dadgar, and A. Strittmatter, "Two charge states of the C_N acceptor in GaN: Evidence from photoluminescence", Phys. Rev. B **98**, 125207 (2018).

[30] M. A. Reshchikov, "Measurement and analysis of photoluminescence in GaN", J. Appl. Phys. **129**, 121101 (2021).

[31] M. Vorobiov, O. Andrieiev, D. O. Demchenko, and M. A. Reshchikov, "Point defects in beryllium-doped GaN", Phys. Rev B **104**, 245203 (2021).

[32] M. A. Reshchikov, D. O. Demchenko, J. D. McNamara, S. Fernández-Garrido, and R. Calarco, "Green luminescence in Mg-doped GaN", Phys. Rev. B **90**, 035207 (2014).

[33] M. A. Reshchikov, "Mechanisms of thermal quenching of defect-related luminescence in semiconductors", Phys. Stat. Sol. A 2000101 (2020).

[34] H. Teisseyre, J. L. Lyons, A. Kaminska, D. Jankowski, D. Jarosz, M. Boćkowski, A. Suchocki, and C. G. Van de Walle, J. Phys. D: Appl. Phys. **50**, 22LT03 (2017).

[35] M. Lamprecht, K. Thonke, H. Teisseyre, and M. Bockowski, "Extremely Slow Decay of Yellow Luminescence in Be-Doped GaN and Its Identification", Phys. Stat. Sol. B **255**, 1800126 (2018).

[36] M. A. Reshchikov and H. Morkoç, "Luminescence properties of defects in GaN", J. Appl. Phys. **97**, 061301 (2005).

[37] M. Vorobiov, O. Andrieiev, D. Demchenko, and M. A. Reshchikov, unpublished.

[38] M. A. Reshchikov, "Determination of acceptor concentration in GaN from photoluminescence", Appl. Phys. Lett. **88**, 202104 (2006).

[39] M. A. Reshchikov, A. Usikov, H. Helava, Yu. Makarov, V. Prozheeva, I. Makkonen, F. Tuomisto, J. H. Leach, and K. Udwary, "Evaluation of the concentration of point defects in GaN", Scientific Reports **7**, 9297 (2017).

[40] H. Sakurai, T. Narita, K. Kataoka, K. Hirukawa, K. Sumida, S. Yamada, K. Sierakowski, M. Horita, N. Ikarashi, M. Bockowski, J. Suda, and T. Kachi, "Effects of the sequential implantation of Mg and N ions into GaN for p-type doping", Appl. Phys. Express **14**, 111001 (2021).

[41] K. Shima, R. Tanaka, S. Takashima, K. Ueno, M. Edo, K. Kojima, A. Uedono, S. Ishibashi, and S. F. Chichibu, "Improved minority carrier lifetime in p-type GaN segments prepared by vacancy-guided redistribution of Mg", Appl. Phys. Lett. **119**, 182106 (2021).

[42] V. Meyers, E. Rocco, K. Hogan, B. McEwen, M. Shevelev, V. Sklyar, K. Jones, M. Derenge, and F. Shahedipour-Sandvik, "P-type conductivity and suppression of green luminescence in Mg/N co-implanted GaN by gyrotron microwave annealing", J. Appl. Phys. **130**, 085704 (2021); doi: 10.1063/5.0049101

[43] M. Takahashi, A. Tanaka, Y. Ando, H. Watanabe, M. Deki, M. Kushimoto, S. Nitta, Y. Honda, K. Shima, K. Kojima, S. F. Chichibu, K. J. Chen, and H. Amano, "Suppression of Green Luminescence of Mg-Ion-Implanted GaN by Subsequent Implantation of Fluorine Ions at High Temperature.", Phys. Stat. Sol. B **257**, 1900554 (2020).